Mechanical Properties of Nanocomposite Cement Incorporating Surface-Treated and Untreated Carbon Nanotubes and Carbon Nanofibers

Rashid K. Abu Al-Rub[1]; Bryan M. Tyson[2]; Ardavan Yazdanbakhsh[3]; and Zachary Grasley[4]

Abstract: To study the effects of functionalized carbon nanotubes (CNTs) and carbon nanofibers (CNFs) on the mechanical properties of cement composites, both untreated and treated CNFs and CNTs were added to cement paste in concentrations of 0.1% and 0.2% by weight of cement. The surface-treated nanofilaments were functionalized in a solution of sulfuric acid (H_2SO_4) and nitric acid (HNO_3). The nanofilaments were dispersed by using an ultrasonic mixer and were then cast into molds. Each specimen was tested in a custom-made three-point flexural test fixture to record the mechanical properties (i.e., the Young's modulus, flexural strength, ductility, and modulus of toughness) at the age of 7, 14, and 28 days. The microstructure was analyzed by using a scanning electron microscope. Untreated CNTs and CNFs were found to enhance the mechanical properties of cementitious materials, whereas the acid-treated CNTs and CNFs degraded the mechanical properties. **DOI:** 10.1061/(ASCE)NM.2153-5477.0000041. *© 2012 American Society of Civil Engineers.*

Introduction

Because of their exceptional stiffness and strength, carbon nanotubes (CNTs) and carbon (CNFs) have been the subject of increasing interest in the reinforcement of many new composite materials. However, research focused on their incorporation in cementitious materials has been limited (Cwirzen et al. 2008a, b; Li et al. 2005; Li et al. 2007; Li et al. 2008a, b; Makar and Beaudoin 2003; Makar et al. 2005; Musso et al. 2009; Nasibulin et al. 2009; Wansom et al. 2006). Recently, experimental tests have shown CNFs to have a Young's modulus as high as 400 GPa, with a tensile strength of 7 GPa (Zhou et al. 2009). Alternatively, CNTs are much stronger and have a Young's modulus around 1 TPa, a tensile strength of 60 GPa, and an ultimate strain capacity of 12% (Yu et al. 2000). The outstanding mechanical properties of CNTs have quickly made them one of the most promising nanomaterials ever produced. If one compares CNTs with steel, CNTs have a modulus of elasticity that is approximately 5 times higher and a tensile strength that is 100 times larger; in addition, CNTs can reach elastic strains 60 times greater than that of steel and yet have a specific gravity one-sixth that of steel. Overall, CNTs are classified into two main categories: single-walled carbon nanotubes (SWCNTs)

and multiwalled carbon nanotubes (MWCNTs). The SWCNTs are composed of a single graphene sheet rolled into a long hollow cylinder, whereas MWCNTs (and also CNFs) are nested arrays of graphene.

Carbon nanotubes are typically formed by catalytic decomposition, whereas common methods to produce CNTs include arc discharge, laser ablation, and chemical vapor deposition (CVD) (Mamalis et al. 2004). On an industrial scale, CVD is the most widely used method to produce CNTs because of its low cost-unit ratio. However, CVD also is associated with higher numbers of defects when compared with other production methods (Coleman et al. 2006). The strength of CNTs is directly dependent on the number of lattice defects. Although defect-free CNTs are desirable in maximizing many properties, such as mechanical, thermal, and electrical attributes, they can hinder bonding within the cement matrix. Defect-free CNTs will simply pull out of cement with minimal effort. Lattice defect sites on CNTs provide a location for the formation of functional groups such as carboxyl (–COOH), and hydroxyl (–OH) groups. The presence of functional groups plays a key role in reinforcing nanocomposites by providing a strong chemical bond between the CNT and the cementitious matrix (Li et al. 2005). Untreated carbon nanofilaments are known to be very hydrophobic, and their high van der Waals force causes them to rapidly agglomerate (i.e., form bundles) when dispersed in water without any surfactant. Two methods are commonly used to enhance the long-term dispersion of nanofilaments within aqueous solutions: application of chemical surfactants and acid functionalization (Vaisman et al. 2006).

Typical acid functionalization uses two highly concentrated acids. The first is nitric acid (HNO_3), which oxidizes the surface, and the second is sulfuric acid (H_2SO_4), which "roughens" the surface. When the surface of a nanofilament is roughened, the carbon-carbon bonds are broken, creating defect sites. This allows the nitric acid to create functional groups on the surfaces of the nanofilaments. Varying the ratio of nitric to sulfuric acid will either increase or decrease the amount of functionalization (Ago et al. 1999;

[1]Assistant Professor, Zachary Dept. of Civil Engineering, Texas A&M Univ., College Station, TX 77843 (corresponding author). E-mail: rabualrub@civil.tamu.edu

[2]Ph.D. Candidate, Zachary Dept. of Civil Engineering, Texas A&M Univ., College Station, TX 77843.

[3]Ph.D. Candidate, Zachary Dept. of Civil Engineering, Texas A&M Univ., College Station, TX 77843.

[4]Assistant Professor, Zachary Dept. of Civil Engineering, Texas A&M Univ., College Station, TX 77843.

Bahr and Tour 2002; Datsyuk et al. 2008; Lakshminarayanan et al. 2004; Zhang et al. 2008). However, increasing the degree of functionalization by changing the ratio of nitric to sulfuric acid will hinder the performance of the nanofilaments. When the amount of sulfuric acid is increased, the surface becomes rougher. This roughness is what allows the functional groups to bond; however, the rougher the surface, the weaker the nanofilaments. Another negative side effect of sulfuric acid is its ability to dissolve through sections of the nanofilaments. This cuts the nanofilaments into smaller lengths, reducing their aspect ratios.

In this research, cement paste was reinforced with both untreated and acid-treated CNTs and CNFs at concentrations of 0.1% and 0.2% by weight of cement. The flexural strength of the batches was compared by using a custom-built three-point bending frame. A scanning electron microscope (SEM) was used to analyze the microstructure of the fractured surfaces.

Experimental Setup

Materials

The cement used for the tests was a commercially available Type I/II portland cement. Previous work (Tyson et al. 2009; Yazdanbakhsh et al. 2009) has shown that a commercial superplasticizer, a high-range polycarboxylate-based, water-reducing ADVA Cast 575 admixture from Grace Corporation, works well to disperse the nanofilaments with minimal effect on the hydration time of the cement paste. The CNTs were NC7000 MWCNTs supplied by Nanocyl, which are produced by a catalytic carbon vapor deposition (CCVD) process. They had a well-controlled diameter of 9.5 nm and an average length of 1.5 μm, with an average aspect ratio of 150. The CNFs were Pyrograf III nanofibers from Applied Sciences, Inc., with a diameter ranging from 60 to 150 nm and a length of 30–100 μm. The CNFs had an average aspect ratio (length to diameter) greater than 1000. Table 1 summarizes the physical properties of the CNFs and CNTs.

Surface Functionalization of the Nanofilaments

Functionalization of the nanofilaments was carried out using the following method: First, 0.9 g of either CNTs or CNFs was added to 300 mL of a solution with a sulfuric to nitric acid ratio of 2:1. The solution was refluxed for 1 h at 85°C and continuously stirred with a magnetic stirrer. After refluxing, the solution was diluted in 4 L of distilled water. The temperature was checked to ensure that the solution was less than 35°C before filtering. Once cool enough, the solution was filtered through a Teflon membrane with a 0.45-μm pore size. The remaining solution was then washed with water and filtered again until it reached a neutral pH. After all the acid was washed from the surface of the nanofilaments, the remaining solution was dried in an oven at 60°C and at a relative humidity of less than 5% for at least 24 hours, or until all the water had evaporated.

Table 1. Physical Properties of Carbon Nanotubes and Carbon Nanofibers

	CNFs	CNTs
Diameter	60–150 nm	9.5 nm
Length	30–100 μm	1.5 μm
Specific surface area	50–60 m^2/g	250–300 m^2/g
Purity	$\geq 90\%$	$\geq 90\%$

Table 2. Mix Design of the Test Specimens

Test specimens	Water/cement ratio	Untreated CNFs: % by weight of cement	Treated CNFs: % by weight of cement	Untreated CNTs: % by weight of cement	Treated CNTs: % by weight of cement
Reference	0.4	0	0	0	0
UF1	0.4	0.1	0	0	0
TF1	0.4	0	0.1	0	0
UF2	0.4	0.2	0	0	0
TF2	0.4	0	0.2	0	0
UT1	0.4	0	0	0.1	0
TT1	0.4	0	0	0	0.1
UT2	0.4	0	0	0.2	0
TT2	0.4	0	0	0	0.2

Preparation and Testing

A total of nine batches of cement specimens were produced. These included a reference sample of plain cement paste, two batches each of cement paste with untreated and treated CNTs at 0.1% and 0.2% by weight of dry cement, and two batches each of cement paste with untreated and treated CNFs at 0.1% and 0.2%. Table 2 summarizes the composition of the nine batches. These batches were labeled to indicate the components and their concentrations. In the labels (see first column of Table 2), the first letter U or T indicates whether the samples were untreated or treated, respectively. In the second position, the letter F represents CNFs and T represents CNTs; in the third position, 1 and 2 indicate nanofilament dosages of 0.1% by weight and 0.2% by weight with respect to dry cement powder, respectively. All five batches had a water to cement ratio of 0.40, and the batches containing either untreated or treated CNTs or CNFs had a surfactant (i.e., superplasticizer) to cement ratio of 0.005. No surfactant was used for the plain cement samples. A minimum of four replications were made for each nanocomposite tested.

To prepare each sample, the CNTs or the CNFs were first mixed with the water and superplasticizer and then placed in an ultrasonic mixer (i.e., ultrasonic vibrations were used to break up agglomerations). The CNTs were mixed for 20 min, and the CNFs were mixed for 10 min. After ultrasonic mixing, the aqueous solution was added to the cement powder in a high-speed rotary mixer and mixed for 7 min. The paste was then placed inside a vacuum chamber for 3 min to remove large air voids. Next, the samples were poured into acrylic molds (6.5 × 6.5 × 160 mm^3) and an electric vibrator was used to ensure good compaction. All samples were demolded after 24 h and cured in a lime-saturated bath until testing. Specimens were tested at 7, 14, and 28 days.

The force and displacement from the three-point flexural tests were converted to stress and strain by using simple strength of materials relations for a three-point bending beam such that

$$\sigma = \frac{3PL}{2bd^2} \qquad (1)$$

and

$$\varepsilon = \frac{6Dd}{L^2} \qquad (2)$$

where P = force (from the load cell); L = length (160 mm); b and d = width and depth (6.5 mm each); and D = displacement (from the LVDT).

After the mechanical tests, random samples were taken to observe the microstructure under the SEM. The fracture surfaces were

cut into approximately 1 mm × 1 mm × 0.5 mm samples and coated with a 3-nm-thick platinum/palladium layer to enhance surface conductivity. Each sample was observed under a JEOL Ltd. JSM-7500F, an ultra-high-resolution field emission scanning electron microscope (FE-SEM).

Results and Discussion

Workability and Hydration of Cement Paste

The workability of the cement paste was greatly affected by the presence of the nanofilaments, especially the untreated CNTs. The presence of the untreated CNTs at 0.2% by weight produced a very viscous solution when mixed with the water and surfactant. Once added to the cement, the solution proved to be challenging to pour into the molds because there was insufficient surfactant to properly disperse the CNTs. However, the addition of more surfactant can lead to delayed hydration of the cement paste (Cwirzen et al. 2008b). The other batches of untreated nanofilaments caused only slight changes in the workability of the cement paste.

Incorporation of the treated CNTs at 0.2% by weight produced an increase in workability when compared with the previously mentioned untreated CNTs. This increase in workability is attributed to the increased wettability caused by the functional groups (–COOH and –OH). As a result, less surfactant was consumed by the nanofilaments, which left more available for the cement. When compared with the plain cement sample, the addition of surfactant or either treated or untreated nanofilaments did not affect hydration time.

Mechanical Properties

The maximum displacement at failure for all nine batches with respect to age was shown in Fig. 1. At 28 days, the largest increase in
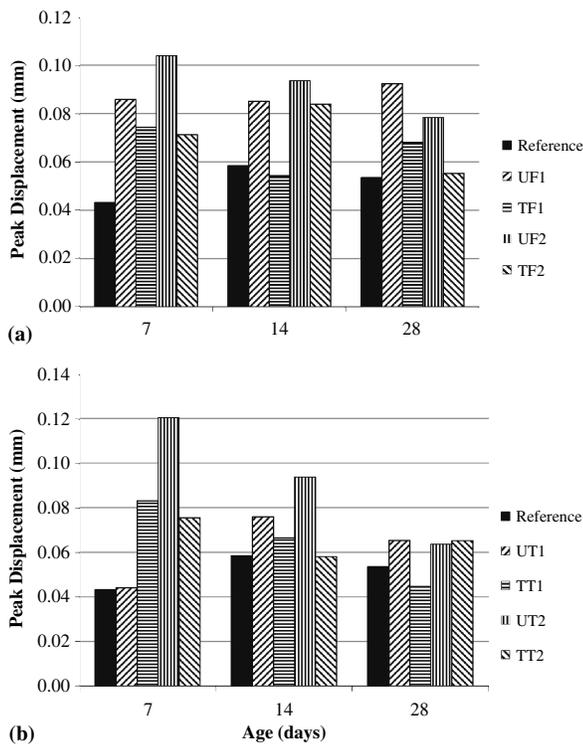
displacement was achieved by the untreated nanofibers UF1, with a 73% increase compared to the reference sample. The largest increase in displacement from the treated nanofilaments was observed with TF1 at 23%. In almost all cases, the untreated nanofilaments outperformed the acid-treated batches. Fig. 2 plots the average peak flexural strength with respect to age. The strength increased as much as 60% for the untreated fibers UF1 at 28 days; however, at 14 and 28 days, the functionalized nanofilaments all showed significant drops in strength compared with the reference sample. In some cases, the drop for the treated nanofibers was as high as 83%. Fig. 3 shows the Young's moduli at 7, 14, and 28 days. As with the flexural strength, a noticeable drop in stiffness can be seen with the treated nanofilaments. The acid-treated samples showed drops as high as 66%, whereas the untreated samples had a 25% increase in stiffness. Fig. 4 shows the average modulus of toughness from all batches, which was calculated as the total area under the stress-strain diagrams. The modulus of toughness shows the same general trends: a worsening effect from the acid-treated nanofilaments and an improvement from the untreated nanofilaments. The untreated CNFs improved the modulus of toughness by 170% at 28 days, whereas the treated CNFs underwent an 83% drop in the modulus of toughness at 28 days.

These results clearly show a drop in mechanical properties when acid-treated nanofilaments are compared with untreated filaments. The reduction in mechanical properties was observed to be time dependent. For all mechanical properties, the 7-day test showed comparable results between the reference sample and both the treated and untreated nanofilaments. However, at 14 days, the mechanical properties of the acid-treated nanofilaments started to degrade. This degradation leveled off between days 14 and 28, which suggests that most of the decay occurred between days 7 and 14. This degradation in mechanical properties for the acid-treated samples can be attributed to the formation of ettringite crystals, which is supported by the SEM images outlined in the following section. Ettringite, an expansive crystalline material, is a
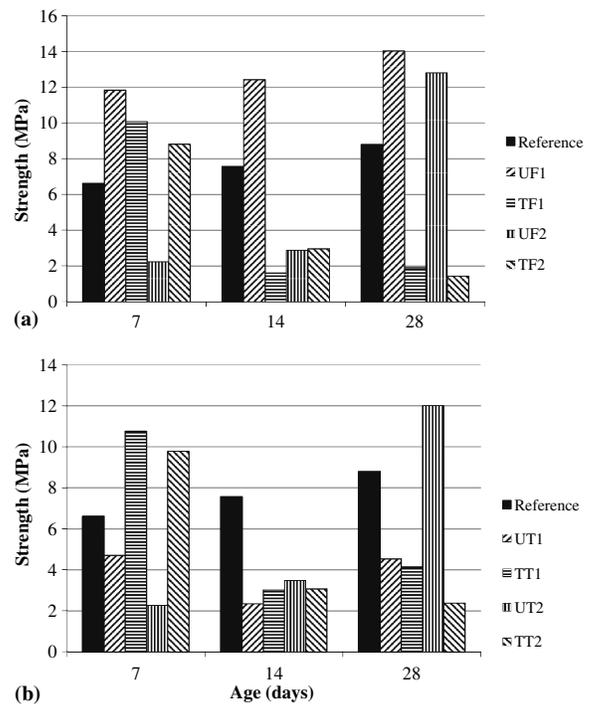

Fig. 1. Peak displacement for both untreated and treated nanofilaments: (a) carbon nanofibers; (b) carbon nanotubes

Fig. 2. Max strength for both untreated and treated nanofilaments: (a) carbon nanofibers; (b) carbon nanotubes

hexacalcium aluminate trisulfate hydrate $[(CaO)_3(Al_2O_3)(CaSO_4)_3 \cdot 32H_2O]$ that is typically caused by the reaction of calcium aluminate with calcium sulfate. However, work by Taylor et al. (2001) has shown that the presence of sulfates within a hydrating cement paste can also lead to excessive ettringite formation. The formation of ettringite then causes the mechanical properties of
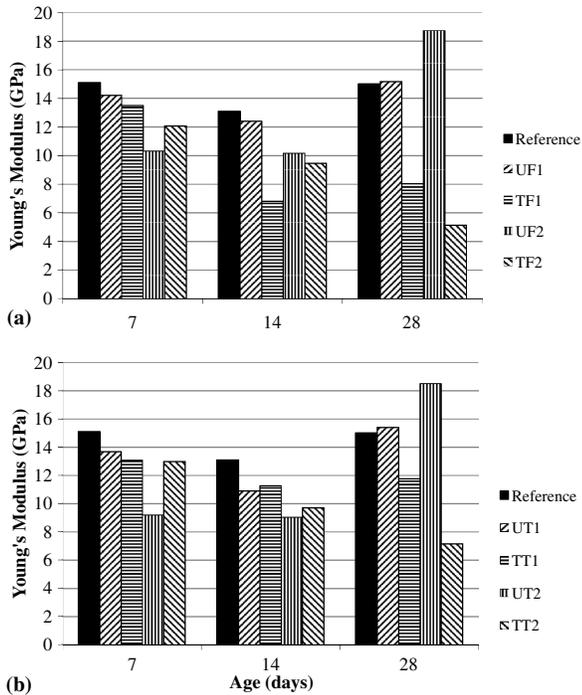
Fig. 3. Young's modulus for both untreated and treated nanofilaments: (a) carbon nanofibers; (b) carbon nanotubes
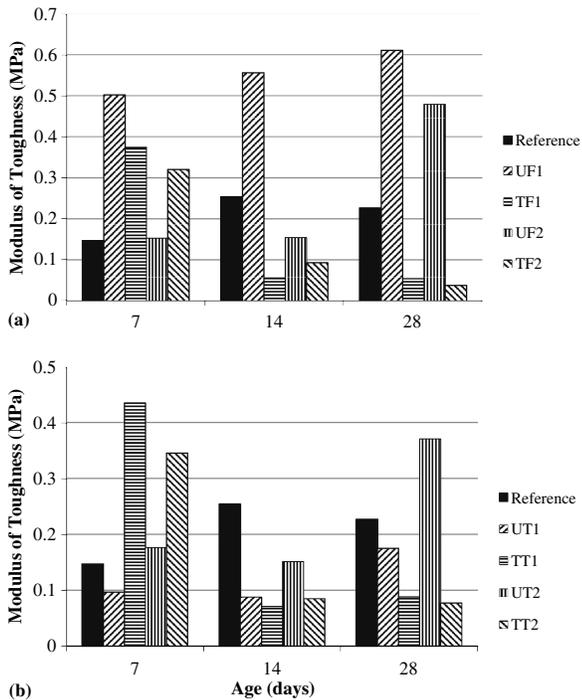
Fig. 4. Modulus of toughness for both untreated and treated nanofilaments: (a) carbon nanofibers; (b) carbon nanotubes

the cement paste to degrade. Sulfate ions left over from the acid-treated nanofilaments may have been on the surface or even inside the hollow tubes and fibers, even though the filaments were washed with distilled water until they reached a neutral pH. During the hydration of the cement, the sulfates were drawn into the solution and then reacted with the hydrating cement paste to form ettringite. This localized reaction explains why the ettringite formations were commonly observed around the embedded nanofilaments. Another possible reason for this observed degradation, proposed by Sanchez and Borwankar (2010), is that preferential leaching and decalcification at the interface of the fiber causes debonding. Decalcification typically occurs in the presence of acidic water, and it causes localized debonding. This debonding it causes a reduction in strength as well as a change in the failure mode from brittle to ductile.

It is noteworthy that the data in Figs. 1–4 have an experimental error, which is always going to be present to some degree in experimental data. This by no means indicates that the experimental results are inconsistent. This error was also observed in many previous studies on the integration of CNTs and CNFs in cementitious materials (e.g., Cwirzen et al. 2008b; Sanchez and Borwankar 2010). The fact that nano-reinforced composites do not always provide "consistent results" can be applied to other studies such as Makar et al. (2005), which examined the hardness of CNT-cement composites over time. Regarding CNT-polymer composites, Chen et al. (2006) used only five different batches to show that when the concentration of CNTs is increased, the strength will decrease, then increase, then decrease again. However, to eliminate the inconsistency within experimental data over time, numerous authors who have published papers on nano-reinforced cement composites have showed data at only one age (e.g., Li et al. 2008b; Musso et al. 2009; Nasibulin et al. 2009). This study, however, generated data at multiple time points so that age-based data could be gathered. Therefore, the current study is very systematic and novel compared with the limited studies in the literature. The presented data show that the hydration of cement paste is very complex and that many factors affecting both the hydration and the interfacial mechanical properties between the matrix and the nanofilaments. In the present work, the surface-treated nanofilaments reduced the mechanical properties because of the surface functionalization.
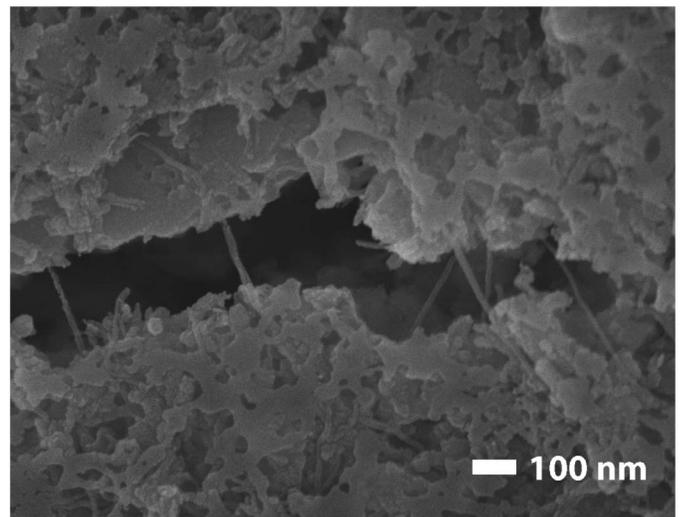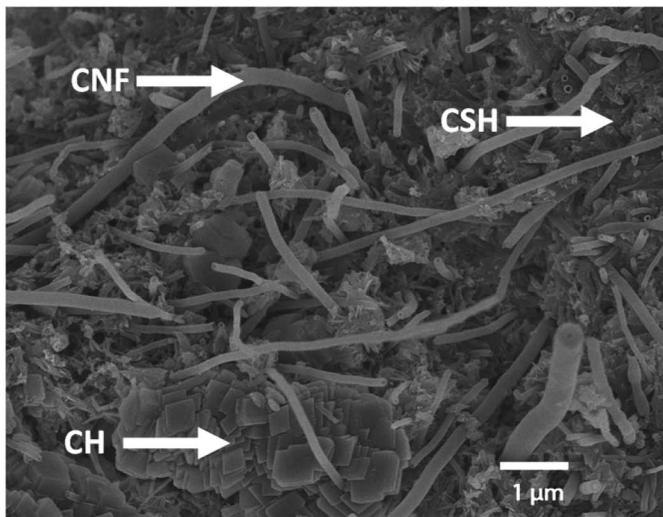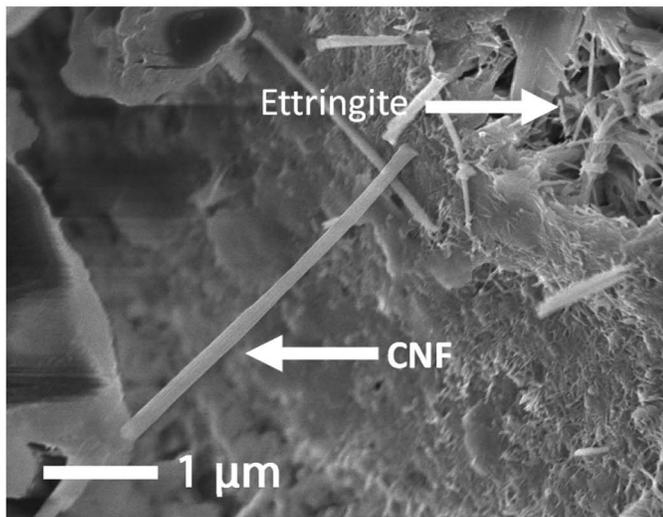
Fig. 5. Untreated CNTs embedded in cement paste bridging a nano-sized crack

(a)

(b)

Fig. 6. SEM image showing the different phases of cement: (a) C-S-H and CH along with CNFs; (b) CNF and ettringite formations

SEM Observations

Fig. 5 shows the bridging of a nano-sized crack by CNTs. The CNTs have a diameter of approximately 10 nm, but they can bridge large cracks because of their high aspect ratio. Fig. 6 shows the fracture surface of the sample containing untreated CNFs at 0.1% by weight [see Fig. 6(a)] and treated CNFs at 0.1% by weight [see Fig. 6(b)]. The CNFs in Fig. 6(a) are bundled together, and it is worth noting that large areas of the fracture surface contain no visible CNFs or CNTs. Fig. 6(b) shows both CNFs and small needle-like ettringite formations, which could explain the degradation in mechanical properties observed with the acid-treated nanofilaments. Fig. 7 shows a bundle of treated CNFs, with the functionalized CNFs bearing a surface coating of hydration products. The hydration products indicate that the interfacial bond between the cement matrix and the CNFs has increased because of the increase in surface functionalization of the acid-treated filaments. Thus, one might expect that the mechanical properties of the treated nanocomposite samples would increase. However, as previously noted, cement samples embedded with functionalized nanofilaments experienced weakened mechanical properties. This weakening effect caused by the ettringite overpowers the increase in strength caused by the enhancement of the interfacial bond.
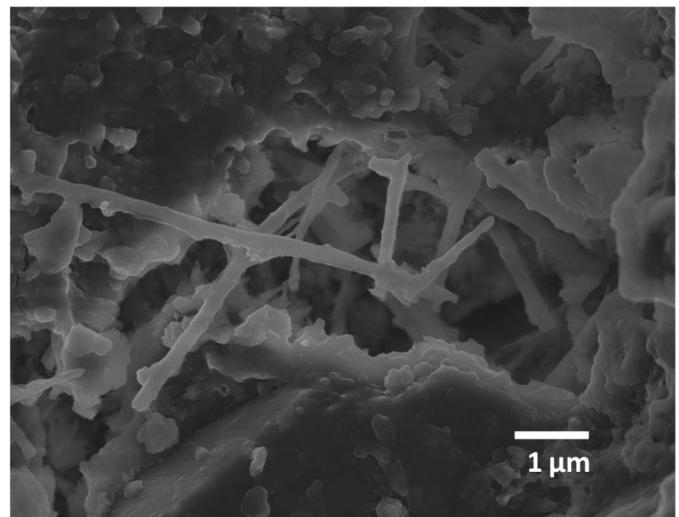

Fig. 7. SEM image of treated CNFs embedded in cement paste

Conclusions

In this study, both treated and untreated CNFs and CNTs were added to cement paste to study how the nanofilaments enhance the mechanical properties of the admixtures. The treated nanofilaments were functionalized in a solution of acid and washed clean before their incorporation in the cement paste. The nanofilaments were well dispersed within aqueous solutions with the help of a chemical surfactant and ultrasonic mixing. The nanofilaments were added to cement paste in concentrations of 0.1% and 0.2% by weight of dry cement. The following data were noted with the cement paste when compared with the plain cement at 28 days: the average ductility increased up to 73%, the average flexural strength increased up to 60%, the average Young's modulus increased up to 25%, and the average modulus of toughness increased up to 170%. These enhancements indicate the presence of interfacial bonds between the nanofilaments and cement, which improved the mechanical properties of the cement paste. However, these enhancements were observed only for untreated nanofilaments. In general, acid-treated nanofilaments had weaker mechanical properties. This degradation in mechanical properties is attributed to the excessive formation of ettringite caused by the presence of sulfates.

In this study, 0.1% by weight and 0.2% by weight concentrations were tested to see how well both treated and untreated nanofilaments perform within the cement paste. From the results of this study, one might be able to limit the range of nanofilament concentrations to find the optimal amount for successfully reinforcing cement paste. The 0.2% by weight concentration might be considered a high concentration to be used for cement paste with high-aspect ratio nanofilaments. Therefore, it is recommended that a nanofilament concentration around 0.1% by weight is a reasonable value for achieving a better dispersion for nanofilaments with relatively high aspect ratios.

Although, useful qualitative comparisons can be obtained from the SEM characterizations, additional microstructural characterization is needed to fully understand the reasons for the degradation or enhancement of the mechanical properties of cementitious nanocomposites reinforced with nanofilaments. Moreover, multiscale nanomechanics-based computational methods and simulations that can be used to explore the key reinforcing mechanisms of nanofilaments in cementious materials are greatly needed.

Acknowledgments

References

Ago, H., et al. (1999). "Work functions and surface functional groups of multiwall carbon nanotubes." *J. Phys. Chem. B*, 103(38), 8116–8121.

Bahr, J. L., and Tour, J. M. (2002). "Covalent chemistry of single-wall carbon nanotubes." *J. Mater. Chem.*, 12(7), 1952–1958.

Coleman, J. N., Khan, U., Blau, W. J., and Gun'ko, Y. K. (2006). "Small but strong: A review of the mechanical properties of carbon nanotube-polymer composites." *Carbon*, 44(9), 1624–1652.

Cwirzen, A., Habermehl-Cwirzen, K., Nasibulin, A. G., Kaupinen, E. I., Mudimela, P. R., and Penttala, V. (2008a). "SEM/AFM studies of cementitious binder modified by MWCNT and nano-sized Fe needles." *Mater. Charact, 60(7)*, 735–740.

Cwirzen, A., Habermehl-Cwirzen, K., and Penttala, V. (2008b). "Surface decoration of carbon nanotubes and mechanical properties of cement/carbon nanotube composites." *Adv. Cem. Res.*, 20(2), 65–73.

Datsyuk, V., et al. (2008). "Chemical oxidation of multiwalled carbon nanotubes." *Carbon*, 46(6), 833–840.

Lakshminarayanan, P. V., Toghiani, H., and Pittman, C. U., Jr (2004). "Nitric acid oxidation of vapor grown carbon nanofibers." *Carbon*, 42(12–13), 2433–2442.

Li, G. Y., Wang, P. M., and Zhao, X. (2005). "Mechanical behavior and microstructure of cement composites incorporating surface-treated multi-walled carbon nanotubes." *Carbon*, 43(6), 1239–1245.

Li, G. Y., Wang, P. M., and Zhao, X. (2007). "Pressure-sensitive properties and microstructure of carbon nanotube reinforced cement composites." *Cem. Concr. Compos.*, 29(5), 377–382.

Li, K.-Z., Wang, C., Li, H.-J., Li, X.-T., Ouyang, H.-B., and Wei, J. (2008a). "Effect of chemical vapor deposition treatment of carbon fibers on the reflectivity of carbon fiber-reinforced cement-based composites." *Compos. Sci. Technol.*, 68(5), 1105–1114.

Li, S. Q., Wang, F., Wang, Y., Wang, J. W., Ma, J., and Xiao, J. (2008b). "Effect of acid and TETA modification on mechanical properties of MWCNTs/epoxy composites." *J. Mater. Sci.*, 43(8), 2653–2658.

Makar, J. M., and Beaudoin, J. J. (2003). "Carbon nanotubes and their application in the construction industry." *Proc., 1st Int. Symp. on Nanotechnology in Construction*, Institute for Research in Construction, National Research Council Canada, Ottawa, ON, 331–341.

Makar, J. M., Margeson, J. C., and Luh, J. (2005). "Carbon nanotube/cement composite—early results and potential applications." *Proc., 3rd Int. Conf. on Construction Materials: Performance, Innovation and Structural Implications*, Institute for Research in Construction, National Research Council Canada, Ottawa, ON, 1–10.

Mamalis, A. G., Vogtländer, L. O. G., and Markopoulos, A. (2004). "Nanotechnology and nanostructured materials: trends in carbon nanotubes." *Precis. Eng.*, 28(1), 16–30.

Musso, S., Tulliani, J.-M., Ferro, G., and Tagliaferro, A. (2009). "Influence of carbon nanotubes structure on the mechanical behavior of cement composites." *Compos. Sci. Technol.*, 69(11–12), 1985–1990.

Nasibulin, A. G., et al. (2009). "A novel cement-based hybrid material." *New J. Phys.*, 11, 11.

Sanchez, F., and Borwankar, A. (2010). "Multi-scale performance of carbon microfiber reinforced cement-based composites exposed to a decalcifying environment." *Mater. Sci. Eng., A*, 527(13–14), 3151–3158.

Taylor, H. F. W., Famy, C., and Scrivener, K. L. (2001). "Delayed ettringite formation." *Cem. Concr. Res.*, 31(5), 683–693.

Tyson, B. M., Abu Al-Rub, R. K., Yazdanbakhsh, A., and Grasley, Z. (2009). "Carbon nanotubes for enhancing the mechanical properties of cementitious materials." *The 2009 Joint ASCE-ASME-SES Conf. on Mechanics of Materials*, Virginia Polytechnic Institute, Engineering Science and Mechanics, Blacksburg, VA.

Vaisman, L., Wagner, H. D., and Marom, G. (2006). "The role of surfactants in dispersion of carbon nanotubes." *Adv. Colloid Interface Sci.*, 128-130, 37–46.

Wansom, S., Kidner, N. J., Woo, L. Y., and Mason, T. O. (2006). "AC-impedance response of multi-walled carbon nanotube/cement composites." *Cem. Concr. Compos.*, 28(6), 509–519.

Yazdanbakhsh, A., Grasley, Z., Tyson, B., and Abu Al-Rub, R. (2009). "Carbon nanofibers and nanotubes in cementitious materials: Some issues on dispersion and interfacial bond." *ACI Special Publication, V. SP 267*, 21–34.

Yu, M. F., Lourie, O., Dyer, M. J., Moloni, K., Kelly, T. F., and Ruoff, R. S. (2000). "Strength and breaking mechanism of multiwalled carbon nanotubes under tensile load." *Science*, 287(5453), 637–640.

Zhang, G., Sun, S., Yang, D., Dodelet, J.-P., and Sacher, E. (2008). "The surface analytical characterization of carbon fibers functionalized by H2SO4/HNO3 treatment." *Carbon*, 46(2), 196–205.

Zhou, Z. P., et al. (2009). "Development of carbon nanofibers from aligned electrospun polyacrylonitrile nanofiber bundles and characterization of their microstructural, electrical, and mechanical properties." *Polymer*, 50(13), 2999–3006.